Inorg. Chem. **2008**, *47*, 4140−4145

Inorganic Chemistry
Article

Intrinsic Carrier Doping in Antiferromagnetically Interacted Supramolecular Copper Complexes with (Pyrazino)tetrathiafulvalene (Pyra-TTF) as the Ligand, $[Cu^{II}Cl_2(pyra\text{-}TTF)]$ and $(Pyra\text{-}TTF)_2[Cu^{I}_3Cl_4(pyra\text{-}TTF)]$

Shun Ichikawa,*,† Shinya Kimura,†,‡ Kazuyuki Takahashi,† Hatsumi Mori,*,†,‡ Gosuke Yoshida,† Yuichi Manabe,† Masaki Matsuda,† Hiroyuki Tajima,† and Jun-ichi Yamaura†

The Institute for Solid State Physics, The University of Tokyo, Kashiwa, Chiba 277-8581, Japan, and CREST-JST, Japan

Received October 5, 2007

New supramolecular copper complexes with pyrazinotetrathiafulvalene (pyra-TTF) as the ligand, $[Cu^{II}Cl_2(pyra\text{-}TTF)]$ (**1**) and $(pyra\text{-}TTF)_2[Cu^{I}_3Cl_4(pyra\text{-}TTF)]$ (**2**), have been synthesized by the diffusion method. Complex **1** is a black block crystal with a three-dimensional (3-D) supramolecular network; the linear chain $[-Cu^{II}Cl_2-(pyra\text{-}TTF)-]_n$ extends along the *b* axis, where the coordinated pyra-TTF donors are stacked in a head-to-tail and ring-over-bond configuration to construct two-dimensional (2-D) sheets, and between the sheets, there are $C\cdots Cl^-$ or $H\cdots Cl^-$ contacts. Even though the electron spin resonance (ESR) measurement reveals the nearly Cu^{II} state, complex **1** is a semiconductor with $\sigma_{RT} = 1.0 \times 10^{-4}$ S cm^{-1} and $E_a = 0.33$ eV. The high-frequency conductivity measurement also confirmed the intrinsic slight carrier doping from Cu^{II} to the pyra-TTF donor. This slight doping enhances not only the real and imaginary dielectric constants but also the antiferromagnetic interaction between Cu^{II} spins following the 2-D Heisenberg model with $2J = -20$ K. In contrast, complex **2** is a very thin black needle. This needle crystal has two crystallographically independent pyra-TTF molecules, which are coordinated and noncoordinated donors. The coordinated donors composed a supramolecular chain $[Cu^{I}_3Cl_4(pyra\text{-}TTF)^0]_n$, whereas the noncoordinated donors formed conducting α''-type pyra-TTF$^{+0.5}$ sheets. This complex is semiconducting with $\sigma_{RT} = 0.1$ S cm^{-1} and $E_a = 0.15$ eV. Both complexes **1** and **2** demonstrate that the pyra-TTF molecule works not only as an oxidized donor by Cu^{II} to construct conducting sheets but also as a ligand coordinated to a Cu cation to form supramolecuar chains.

Introduction

The synergy or interplay between electrical conductivity, magnetism, permittivity, and optical properties in the use of the spin, charge, lattice, and degrees of freedom of molecules has attracted great interest from fundamental science to potential applications. Among these applications, the use of organic donors containing nitrogen atoms as ligands has been tried with a view toward the creation of new molecular-based multifunctional materials.[1−7] These metal complexes tend to have shorter donor−metal distances than ordinary noncoordination charge transfer complexes because of coordination bonds. So, these systems are expected to exhibit interactions between the π electrons on the organic donors and the magnetic d moment of the metal ions, the so-called π−d interaction. Recently, we were the first to synthesize a three-dimensional (3-D) supramolecular copper(II) complex with pyrazino-fused TTF as the ligand, $[CuCl_2(BP\text{-}TTF)]$ (BP-TTF = bis(pyrazino)tetrathiafulvalene, Figure 1),[8] and the pyrazino-fused TTFs such as BP-TTF could have the shortest donor−metal distance. The π−d interaction of this complex

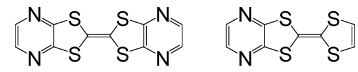

Figure 1. Molecular structures of BP-TTF ($E_1 = 1.05$V vs SCE) and pyra-TTF ($E_2 = 0.68$ V).

* To whom correspondence should be addressed. E-mail: (S.I.) ichikawa@issp.u-tokyo.ac.jp, (H.M.) hmori@issp.u-tokyo.ac.jp. Fax: +81-4-7136-3444.
† The University of Tokyo.
‡ CREST-JST.

10.1021/ic7019632 CCC: $40.75
Published on Web 04/16/2008

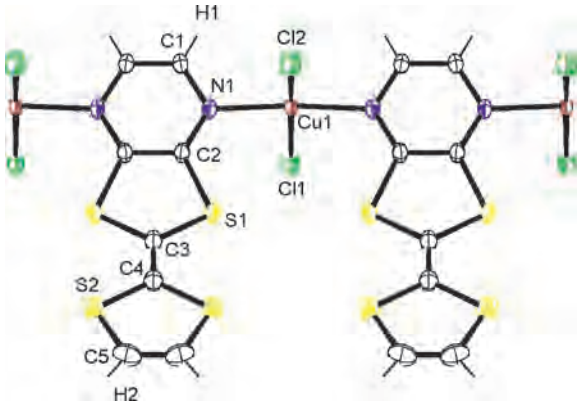

Figure 2. ORTEP drawing and atomic numbering scheme of the donor molecule of **1**.

derives an antiferromagnetic behavior fitted by a Bonner−Fisher model from 2 to 300 K with $S = 1/2$ and $2J = -7$ K between Cu^{II}, mediated by self-assembling donor π columns. However, this complex was an insulator due to the absence of carriers; charge transfer does not occur from TTF moieties to copper ions because of the high first oxidation potential, E_1, of BP-TTF (1.05 V). We therefore selected pyrazinotetrathiafulvalene (pyra-TTF) (Figure 1, $E_1 = 0.68$ V), which is more easily oxidized than BP-TTF, to induce charge transfer from organic donors to copper ions in a complex and synthesized new copper complexes such as $[CuCl_2$(pyra-TTF)] (**1**) and (pyra-TTF)$_2[Cu_3Cl_4$(pyra-TTF)] (**2**). Herein, we report the preparation, the crystal structures, and the magnetic, the electrical, and the dielectric properties of these complexes.

Experimental Section

Synthesis. Pyra-TTF was synthesized as described in the literature.[9−11] Copper complexes **1** and **2** were prepared by a diffusion method; pyra-TTF (10 mg) and TBA_2CuCl_4 (260 mg) in dry ethanol were added to the diffusion cell under a nitrogen atmosphere. After about 2 weeks, black plate crystals of **1** and black needle crystals of **2** were collected by filtration and washed with dry ethanol. The compositions of these complexes were determined by scanning electron microscopy−energy dispersive spectroscopy (SEM-EDS) (JEOL JCM-5000, Oxford WDX 400).

X-ray Analysis of These Complexes. A single crystal of **1** was mounted for data collection at room temperature on a Rigaku7R diffractometer, λ(Mo Kα) = 0.71069 Å. The structure was solved with direct methods and refined with the full-matrix least-squares technique using Crystal Structure (version 3.6.0, Rigaku Co. and Rigaku/MSC). Anisotropic thermal parameters were applied to all non-hydrogen atoms. The hydrogen atoms were generated geometrically (C−H = 0.950 Å). A single crystal of **2** was mounted on a CCD area ditector, Bruker, SMART APEX, λ(Mo Kα) at 150 K. The structure was solved with direct methods and refined with the full-matrix least-squares technique using SHELXL on Crystal Structure (version 3.6.0, Rigaku Co. and Rigaku/MSC). Anisotropic thermal parameters were applied to all non-hydrogen atoms. The hydrogen atoms were generated geometrically (C−H = 0.950 Å).

Resistivity Measurement. The temperature dependencies of the resistivities of single crystals of **1** and **2** were measured by the ac four-terminal method at 27 Hz with 15 μm Au wires attached by carbon paint as contacts.

Electron Spin Resonance (ESR) Measurement. To estimate the oxidation state of Cu in these complexes, the ESR measurement was carried out at 290 K with a Bruker EMS 9.3-GHz X-band ESR spectrometer. The angular dependence of the g value and the line width were measured for complex **1**.

Permittivity Measurement. The temperature dependencies of the real (ε') and the imaginary (ε'') parts of the dielectric constants of the single crystal of **1** were measured by an impedance analyzer (Agilent 4294A) under 1, 10, and 100 kHz and 1 MHz. The measurement was performed by two probes along the c^* axis with 15μm Au wires attached by silver paints at 2−300 K.

Magnetization Measurement. The temperature dependencies of the magnetic susceptibilities for **1** (powder, 5.3 mg) and **2** (powder, 14.8 mg) were investigated by a Quantum Design MPMS-XL superconducting quantum interference device (SQUID) magnetometer under 10 000 Oe at 2−300 K. The diamagnetic core contribution is corrected by Pascal's law.

Results and Discussion

Synthesis of the Complexes. Complexes **1** and **2** were synthesized by diffusion methods with an H-type cell in ethanol, and the ratio for the two kinds of obtained complexes was about 1:1. Other solvents such as methanol, propanol, and dichloromethane were used for the synthesis, but no complex or the poor quality one was obtained in these solvents because of solubility problems. Although the vertical diffusion method, which is a diffusion method with a test tube, was also carried out with several solvents, only poor quality crystals were obtained because of the fast diffusion speed. Therefore, the diffusion method with an H-type cell in ethanol as a solvent is the best way to obtain high quality crystals.

Crystal Structures. The X-ray single crystal analysis of **1** revealed the 3-D supramolecular network. Figure 2 is the ORTEP drawing and the atomic numbering scheme of complex **1**. The linear chain $[-Cu^{II}Cl_2-$(pyra-TTF)$-]_n$ extends along the b axis, where the Cu^{II} atom in a planar geometry is coordinated by two Cl^- and two N atoms of pyra-TTF as ligands (Cu−Cl = 2.2290(16) Å, Cu−N = 2.042(2) Å). The pyra-TTF donors are stacked in a head-to-tail and ring-over-bond configuration, where the pyrazino rings stick out of the donor stacking column (Figure 3a). Figure 3b reveals that the donors do not form uniform

(1) Iwahori, F.; Golhen, S.; Ouahab, L.; Carlier, R.; Suter, J. P. *Inorg. Chem.* **2001**, *40*, 6541–6542.
(2) Jia, C.; Liu, S. X.; Ambrus, C.; Neels, A.; Labat, G.; Decurtins, S. *Inorg. Chem.* **2006**, *45*, 3152–3154.
(3) Setifi, F.; Ouahab, L.; Golhen, S.; Yoshida, Y.; Saito, G. *Inorg. Chem.* **2003**, *42*, 1791–1793.
(4) Kanehama, R.; Umemiya, M.; Iwahori, F.; Miyasaka, H.; Sugiura, K.; Yamashita, M.; Yokochi, Y.; Ito, H.; Kuroda, S.; Kishida, H.; Okamoto, H. *Inorg. Chem.* **2003**, *42*, 7173–7181.
(5) Devic, T.; Batail, P.; Fourmigué, M.; Avarvari, N. *Inorg. Chem.* **2004**, *43*, 3136–3141.
(6) Massue, J.; Bellec, N.; Chopin, S.; Levillain, E.; Roisnel, T.; Clérac, R.; Lorcy, D. *Inorg. Chem.* **2005**, *44*, 8740–8748.
(7) Wang, L.; Zhang, B.; Zhang, J. *Inorg. Chem.* **2006**, *45*, 6860–6863.
(8) Ichikawa, S.; Kimura, S.; Mori, H.; Yoshida, G.; Tajima, H. *Inorg. Chem.* **2006**, *45*, 7575–7577.
(9) Melby, L. R.; Hartzler, H. D.; Sheppard, W. A. *J. Org. Chem.* **1974**, *39*, 2456–2458.
(10) Papavassiliou, G. C.; Yiannopoulos, S. Y.; Zambounis, J. S. *Chem. Scr.* **1987**, *27*, 265–268.
(11) Papavassiliou, G. C.; Gionis, V.; Yiannopoulos, S. Y.; Zambounis, J. S.; Kobayashi, K.; Umemoto, K. *Mol. Cryst. Liq. Cryst.* **1988**, *156*, 277–287.

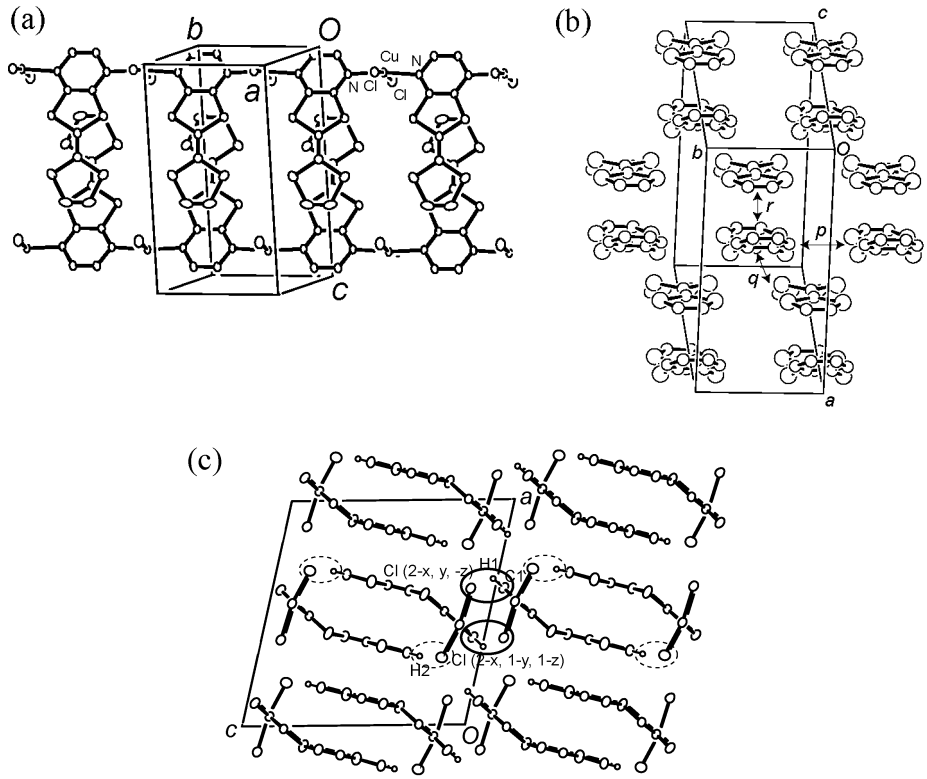

Figure 3. (a) Crystal structure; (b) donor arrangement; (c) structure projected along the *b* axis for **1**. (The C···Cl^- and the H···Cl^- contacts between the pyrazino rings and the Cl^- are shown by circles, and the H···Cl^- contacts between the TTF moiety and the Cl^- are shown by dotted circles.)

Table 1. Crystallographic Data for **1**

formula	$C_8H_4N_2S_4CuCl_2$
fw	390.82
T (K)	293
wavelength (Å)	0.71069
cryst syst	monoclinic
space group	*C*2/*m*
a (Å)	13.802(2)
b (Å)	6.8732(7)
c (Å)	13.314(2)
α (deg)	90.00
β (deg)	103.03(1)
γ (deg)	90.00
V (Å^3)	1230.5(3)
Z	4
D_{calcd} (g cm^{-3})	2.109
R1	0.034
wR2	0.087
GOF	1.008

stacking columns but that two donor units form a honeycomb network. The intermolecular overlap integrals[12] of pyra-TTF including N atoms are calculated on the basis of the molecular orbitals obtained by WinMOPAC (version 3.9.0, Fujitsu Limited) to be $r = 1.78$, $p = 0.538$, and $q = 4.64$ ($\times 10^{-3}$). The largest interaction q is observed in the diagonal direction, and the second largest one r is observed within a unit, so that two-dimensional (2-D) interactions spread in the *ab* plane. In addition, there exist contacts between the donor sheets, C1···Cl ($2 - x$, y, $-z$) (3.354(3) Å), Cl ($2 - x$, y, $-z$)···H1 (2.747(0) Å), and Cl ($2 - x$, $1 - y$, $1 - z$)···H2 (2.6308(0) Å), as shown in Figure 3c. Therefore, this material is the 3-D supramolecular copper(II) complex. Crystallographic data for complex **1** are shown in Table 1.

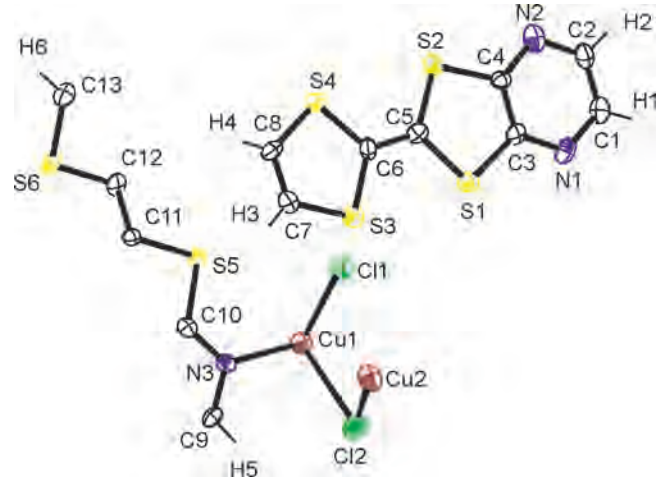

Figure 4. ORTEP drawing and atomic numbering scheme of a donor molecule of **2**.

The X-ray single crystal analysis of **2** shows two different types of pyra-TTF molecules, a coordinated donor and a noncoordinated donor, as shown in Figures 4 and 5a. Their center C═C double bond lengths suggest that the coordinated donor is neutral by 1.33(15) Å and the noncoordinated one is close to +0.5 by 1.361(10) Å as (pyra-$TTF^{+0.5}$)$_2$[Cu_3Cl_4-(pyra-$TTF)^0$].[13–15] Uniform stacks of noncoordinated donors form an α″-type donor arrangement as shown in Figure

(12) Mori, T.; Kobayashi, A.; Sasaki, Y.; Kobayashi, H.; Saito, G.; Inokuchi, H. *Bull. Chem. Soc. Jpn.* **1984**, *57*, 627.

(13) Kobayashi, H.; Kato, R.; Mori, T.; Kobayashi, A.; Sasaki, Y.; Saito, G.; Enoki, T.; Inokuchi, H. *Mol. Cryst. Liq. Cryst.* **1984**, *107*, 33–43.

(14) Guionneau, P.; Kepert, C. J.; Bravic, G.; Chasseau, D.; Truter, M. R.; Kurmoo, M.; Day, P. *Synth. Met.* **1997**, *86*, 1973–1974.

(15) Umland, T. C.; Allie, E.; Kuhlmann, T.; Coppens, P. *J. Phys. Chem.* **1988**, *92*, 6456.

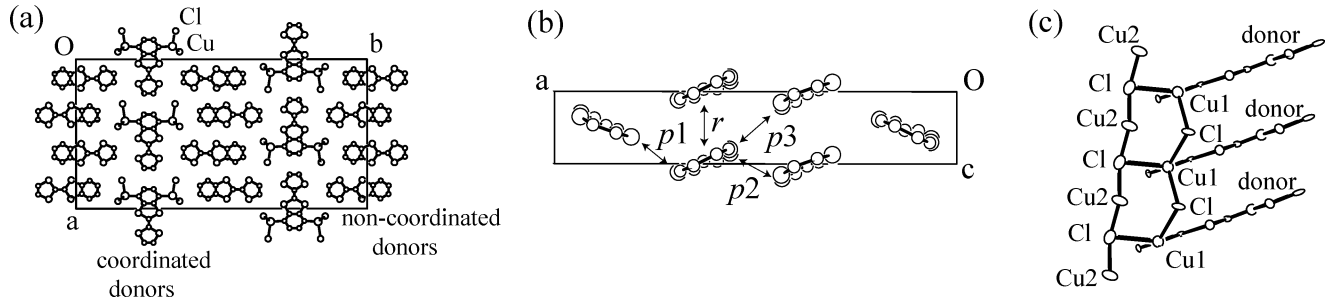

Figure 5. (a) Crystal structure projected along the *c* axis; (b) noncoordinated donor arrangement; (c) chain structure of coordinated donors projected along the *b* axis for **2**.

Table 2. Crystallographic Data for **2**

formula	$C_{24}H_{12}N_6S_{12}Cu_3Cl_4$
fw	1101.57
T (K)	150
wavelength (Å)	0.70550
cryst syst	orthorhombic
space group	*Pnma*
a (Å)	21.387(2)
b (Å)	41.838(5)
c (Å)	3.8011(4)
α (deg)	90.00
β (deg)	90.00
γ (deg)	90.00
V (Å^3)	3401.2(6)
Z	4
D_{calcd} (g cm^{-3})	2.151
R1	0.094
wR2	0.22
GOF	1.020

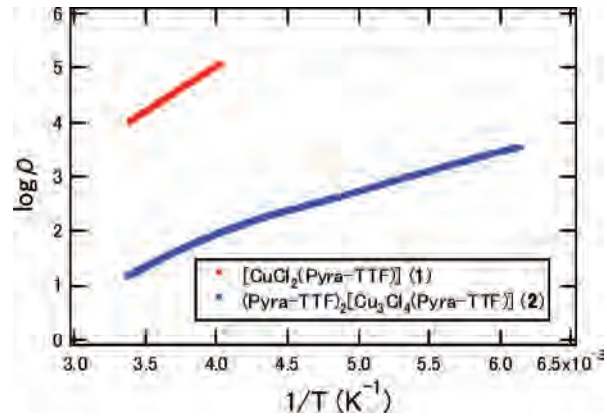

Figure 6. Log ρ vs T^{-1} plots obtained by resistivity measurements for **1** and **2**.

5b.[16–18] The overlap integrals are calculated to be $r = -3.36$, $p1 = -0.252$, $p2 = 0.644$, and $p3 = 2.74$ ($\times 10^{-3}$), suggesting a pseudo-one-dimensional interaction along the *c* axis. In contrast, coordinated donors form one-dimensional (1-D) uniform stacking columns linked by a 5.5-membered ring composed of $Cu^{I}_{2.5}Cl_3$. This column has two kinds of Cu^{I}: one has a tetragonal $Cu1^{I}Cl_3N$ geometry with the full occupancy of Cu1 (1.00), and the other has a bent $Cu2^{I}Cl_2$ geometry with half the occupancy of Cu2 (0.5). Crystallographic data for complex **2** are shown in Table 2.

Resistivity Measurements. The temperature dependencies of the resistivities of the single crystals of **1** and **2** were measured by the ac four-terminal method at 27 Hz with carbon paint contacts, as shown in Figure 6. Because of the intrinsic slight carrier doping from Cu^{II} to the coordinated pyra-TTF, this complex is semiconducting with $\sigma_{RT} = 1.0 \times 10^{-4}$ S cm^{-1} and $E_a = 0.33$ eV, in contrast to the insulating complex [$Cu^{II}Cl_2$(BP-TTF)].[8] Since pyra-TTF has a lower oxidation potential ($E_1 = 0.68$ V vs SCE) than BP-TTF (1.05 V), slight carrier doping occurred. The other complex, **2**, is more conductive, owing to the pyra-TTF$^{+0.5}$ donor columns with $\sigma_{RT} = 0.10$ S cm^{-1} and $E_a = 0.15$ eV.

ESR Measurement. To estimate the oxidation state of Cu in these complexes, the ESR measurement was carried out at 290 K. Figure 7 shows the angular dependence of the *g* value and the line width for the Lorentzian signal for a single crystal of [$CuCl_2$(pyra-TTF)]. The *g* value varies from 2.05 to 2.27 when the crystal is rotated (as seen in Figure 8), and this result is similar to those of [$Cu^{II}Cl_2$(BP-TTF)]. Therefore, the Cu in [$CuCl_2$(pyra-TTF)] is nearby the Cu^{II}. This fact is in agreement with SQUID and X-ray data. So, the semiconducting behavior of **1** might be the intrinsic slight carrier doping from Cu^{II} to the pyra-TTF donors.

The ESR measurement was also carried out for the powder samples of (pyra-TTF)$_2$[Cu_3Cl_4(pyra-TTF)]. A Lorentzian signal was observed with $g = 2.01$ and $\Delta H = 18.1$ G, which is attributed to pyra-TTF$^{\cdot+}$. Therefore, the Cu in (pyra-TTF)$_2$[Cu_3Cl_4(pyra-TTF)] is expected to be Cu^{I}.

Permittivity Measurement. To confirm the intrinsic carrier doping of **1**, the temperature dependencies of the real (ε') and the imaginary (ε'') parts of the dielectric constants of a single crystal of **1** were measured by an impedance analyzer (Agilent 4294A) under 1, 10, and 100 kHz and 1 MHz, as shown in Figure 9. The room temperature ε' and ε'' at 1 kHz are 45 and 2240, respectively. The obtained ac conductivity $\sigma = 2\pi f\varepsilon_0\varepsilon'' = 1.25 \times 10^{-6}$ S cm^{-1} (f = frequency; ε_0 = vacuum permittivity), $E_a = 0.39$ eV, and the frequency dependence implies that carriers of **1** are really doped. Figure 10 shows log ρ versus T^{-1} plots under various frequencies calculated from ε''. All plots follow T^{-1}, which does not indicate the variable range hopping (log $\rho \propto T^{-}$ $(1/d+1)$; d = dimensional system) but intrinsic semiconductors. On the other hand, no dielectric response is observed for the insulating [$CuCl_2$(BP-TTF)][8] without carriers.

Magnetization Measurements. The temperature dependencies of magnetic susceptibilities for **1** and **2** were investigated by a Quantum Design MPMS-XL SQUID magnetometer under 10 000 Oe, as shown in Figure 11. The

(16) Mori, T. *Bull. Chem. Soc. Jpn.* **1998**, *71*, 2509–2526.
(17) Mori, T.; Mori, H.; Tanaka, S. *Bull. Chem. Soc. Jpn.* **1999**, *72*, 179–197.
(18) Mori, T. *Bull. Chem. Soc. Jpn.* **1999**, *72*, 2011–2027.

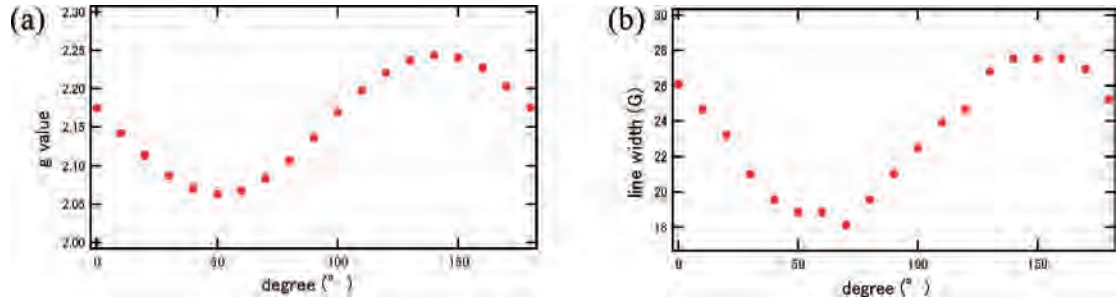

Figure 7. Angular dependencies of (a) the g value and (b) the line width for [$CuCl_2$(pyra-TTF)] (**1**) at 290 K.

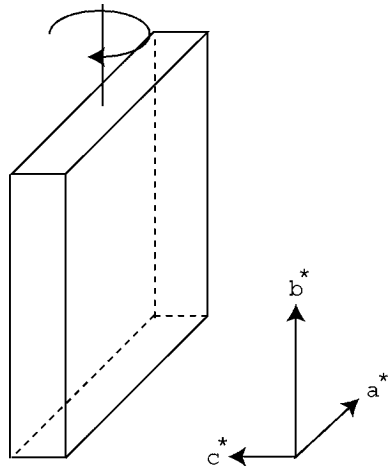

Figure 8. Rotation axis of ESR measurement for **1**.

magnetic susceptibility χ_1 at 300 K after the subtraction of the Pascal diamagnetic contribution is 1.41×10^{-3} emu mol^{-1} and follows the 2-D Heisenberg model from 300 to 4 K with $S = 1/2$ and $2J = -20$ K. The preliminary torque measurement of **1** indicates no long-range magnetic order down to 6 K. The larger antiferromagnetic interaction between Cu^{II} ($S = 1/2$) spins, compared with that of [$CuCl_2$(BP-TTF)], $2J = -7$ K,[8] might be caused not only by the 3-D interaction but also by the slightly doped carriers in the pyra-TTF donors as ligands. In contrast, the magnetic susceptibility χ_2 at 300 K of compound **2** is 9.65×10^{-4} emu mol^{-1} and fits to the Bonner−Fisher model from 300 to 2 K with $S = 1/2$ and $2J = -42$ K.

Intrinsic Carrier Doping. In this study, new supramolecular copper complexes with pyra-TTF as the ligand were synthesized, and the mechanism of semiconducting behaviors of both salts was investigated.

As shown in Figure 7, ESR measurement for complex **1** reveals that the angular dependences of the g values are 2.05−2.27, which are similar to [$Cu^{II}Cl_2$(BP-TTF)^0].[8] In addition, these values are in good agreement with the magnetic susceptibility ($\chi_{rt} = 1.41 \times 10^{-3}$ emu mol^{-1}, $S = {}^1/_2$ (Cu^{II})), and so, the copper ions in complex **1** are close to Cu^{II}. Unlike [$Cu^{II}Cl_2$(BP-TTF)^0], this complex however is not an insulator but rather a semiconductor, with 10^{-4} S cm^{-1} and $E_a = 0.33$ eV. If the copper ions in complex **1** are completely Cu^{II}, then the complex is an insulator due to neutral TTFs. There are three possible mechanisms to explain the semiconducting behavior. The first one is that impurity states appear so that the conducting behavior is observed. In order to check it, the electrical conductivity of complex **1** was measured many times. As a result, the conductivity data were reproducible with $\sigma_{rt} = 10^{-4}$ S cm^{-1} and $E_a = 0.33$ eV (Figure 6). Moreover, the high-frequency conductivities derived from ε'', which can be obtained with permittivity measurement (see the Permittivity Measurement section and Figures 9 and 10), are also reproducible with $\sigma_{rt} = 10^{-6}$ S cm^{-1} and $E_a = 0.39$ eV at 1 kHz. The semiconducting behavior is an intrinsic property, and the mechanism of impurity states is not acceptable, since there is no sample dependence. The second one is that d−π band hybridization occurs; even if the hybridization of the 3d orbital of Cu^{II} and the π band of pyra-TTF occurs, the degree of hybridization is very small, since the conductivity is still low and no metallic behavior could be observed. The third one is that intrinsic carrier doping occurs; the most plausible mechanism is slight hole carrier doping from Cu^{II} to pyra-TTF. The highest occupied molecular orbital (HOMO) level approaches to the 3d orbital of Cu^{II} on the basis of the strategy to reduce an oxidation potential to pyra-TTF ($E_1 =$

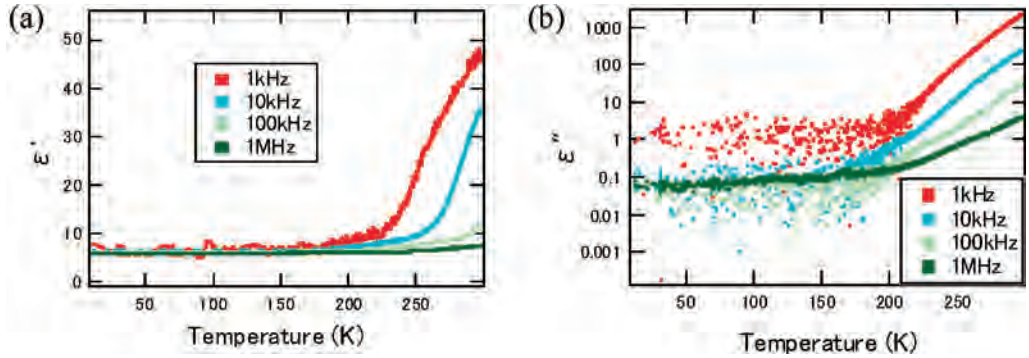

Figure 9. Temperature dependencies of (a) real (ε') and (b) imaginary (ε'') parts of complex dielectric constants of **1** (||c*).

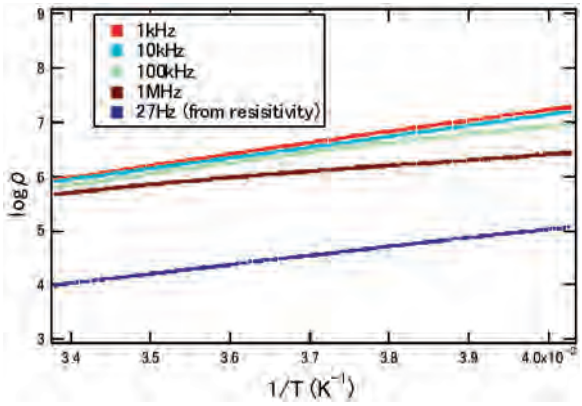

Figure 10. Log ρ vs T^{-1} plots obtained from ε'' for **1**.

0.68 vs SCE) from BP-TTF ($E_1 = 1.05$ vs SCE). As a result, the oxidation state of the copper ions in the complex is not expected to be "completely" Cu^{II} but "close to" Cu^{II}; slight carrier doping occurs, and semiconducting behavior appears in complex **1**.

In complex **2**, $Cu^{II}Cl_2$ also oxidizes pyra-TTF donor molecules to form (pyra-$TTF^{0.5+}$)$_2$[$Cu^{I}_3Cl_4$(pyra-$TTF)^0$]. There are two kinds of pyra-TTF molecules: the neutral one is coordinated to Cu^I toward the supramolecular $(Cu^{I}_{2.5}Cl_3)_n$ chain, and the other, pyra-$TTF^{0.5+}$, is noncoordinated to construct an α''-type conducting sheet.

Therefore, in both complexes **1** and **2**, Cu^{II} oxidizes partially or fully the pyra-TTF donor, namely intrinsic carrier doping, so that the novel antiferromagnetically interacted supramolecular copper complexes were synthesized.

Conclusion

We have synthesized copper complexes with pyra-TTF as the ligand, [$CuCl_2$(pyra-TTF)] (**1**) and (pyra-TTF)$_2$[Cu_3Cl_4-(pyra-TTF)] (**2**). The crystal structure of **1** shows a 3-D supramolecular framework: the 1-D linear coordinated chain [$CuCl_2$(pyra-TTF)]$_n$, the 2-D donor sheet, the C···Cl^-, and two kinds of H···Cl^- contacts between donor sheets. Owing to the intrinsic slight carrier doping from Cu^{II} to a coordinated pyra-TTF, this complex is not an insulator but a semiconductor with $\sigma_{RT} = 1.0 \times 10^{-4}$ S cm^{-1}. The doping enhances the

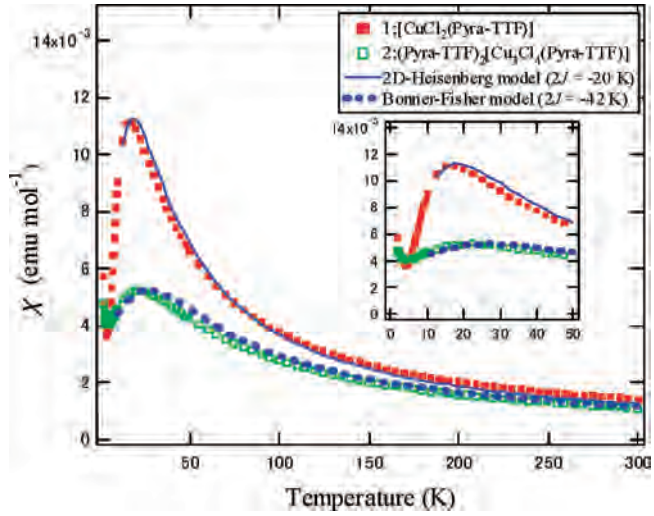

Figure 11. Temperature dependence of magnetic susceptibility for **1** and **2**. The blue dotted line denotes the theoretical fitting for the 1-D Bonner−Fisher model ($H = -2J\sum[S_iS_{i+1}]$)[19] in the temperature range 10.5−300 K; the solid blue line exhibits the theoretical fitting for the 2-D Heisenberg model ($H = -2J\sum[S_iS_j]$)[20] in the temperature range 13.5−300 K.

dielectric constant ($\varepsilon' = 45$; $\varepsilon'' = 2240$) and the antiferromagnetic interaction (2-D Heisenberg model with $2J = -20$ K) between Cu^{II} ions through d−π interactions. On the other hand, compound **2** has two types of pyra-TTF donors (coordinated and noncoordinated), where the 1-D supramolecular chain [Cu_3Cl_4(pyra-TTF)] and the α''-type donor sheet are constructed. The pyra-TTF is a potential donor not only to coordinate to the Cu atom and form a supramolecular chain but also to be oxidized and construct a conducting sheet. The tuning of oxidation potential for the development of magnetic conductors is in progress.

Acknowledgment. This work was supported by the Grants-in-Aid for Scientific Research (No. 17540315) from JSPS (Japan Society for the Promotion of Science) and CREST (Core Research for Evolutional Science and Technology) of JST (Japan Science and Technology Corporation).

Supporting Information Available: X-ray crystallographic data for **1** and **2** in CIF format. This material is available free of charge via the Internet at http://pubs.acs.org.

IC7019632

(19) Bonner, J. C.; Fisher, M. E. *Phys. Rev.* **1964**, *135*, A640–A658.
(20) Lines, M. E. *J. Phys. Chem. Solids* **1970**, *31*, 101.